Acta Metall. Sin. (Engl. Lett.), 2015, **28**(6), 787–792
DOI 10.1007/s40195-015-0264-2

Effects of Sub-zero Celsius Treatment and Tempering on the Stability of Retained Austenite in Bearing Steel

Xiao-Hui Lu · Wei Li · Cheng-Lin Wang · Hong-Shan Zhao · Xue-Jun Jin

Received: 23 December 2014 / Revised: 7 February 2015 / Published online: 21 March 2015

Abstract In this work, the influence of sub-zero Celsius treatment and tempering on the mechanical and thermal stability of retained austenite in bearing steel were assessed by tensile test and DSC. Compared with traditional quenched and tempered treatment, sub-zero Celsius treatment obviously decreases the volume fraction of retained austenite. Moreover, the mechanical stability of retained austenite was enhanced due to the accumulation of compressive stresses in retained austenite after sub-zero Celsius treatment and tempering. Meanwhile, the morphology of retained austenite changed from film-like to blocky with austenitization temperature increasing, and the mechanical stability of film-like retained austenite is higher than that of blocky one. The DSC results showed that the activation energy of retained austenite decomposition slightly increased through sub-zero Celsius treatment and tempering. This result may probably be ascribed to partitioning of carbon during tempering. However, the temperature at which retained austenite starts to decompose is unchanged.

KEY WORDS: Bearing steel; Sub-zero Celsius treatment; Retained austenite; Stability

1 Introduction

GCr15 steel, with high carbon concentrations of (0.9–1.05) wt%, is one of the most widely exploited materials for ball and roller bearings. It is routinely treated by quenched and tempered (QT) heat treatment with microstructures of dominant tempered martensite, a few amounts of retained austenite (RA) and spherical carbides [1, 2]. The RA has a crucial role in determining the fatigue performance and dimensional stability in bearing steel [3]. In operating condition, phase transformation from RA to martensite leads to a deterioration in fatigue performance, because the volume expansion accompanying its transformation introduces localized stresses [4]. Otherwise, the dimensional stability is the most important issue for high precision parts and components, such as aerospace industry and precision machine tools [5].

Sub-zero Celsius treatment as a supplemental process of traditional QT heat treatment is beneficial for the performance of tool steels with respect to dimensional stability [6, 7], wear [8–10], hardness [11, 12] and fatigue [13]. The improvement of mechanical properties is due to a combined effect of transformed RA to martensite and finer transition carbides precipitation [5–13], i.e., the combined results of sub-zero Celsius treatment and tempering. The greatest improvement in mechanical properties is obtained by carrying out the sub-zero Celsius treatment between QT [6].

Sub-zero Celsius treatment [14–16] could be effective to stabilize RA, but the mechanisms remain largely unknown. It is believed that compressive state of stress can stabilize RA

Available online at http://link.springer.com/journal/40195

X.-H. Lu · X.-J. Jin (✉)
State Key Lab of Metal Matrix Composite, School of Materials Science and Engineering, Shanghai Jiao Tong University, Shanghai 200240, China
e-mail: jin@sjtu.edu.cn

X.-H. Lu · W. Li (✉) · C.-L. Wang · H.-S. Zhao
Institute of Advanced Steels and Materials, School of Materials Science and Engineering, Shanghai Jiao Tong University, Shanghai 200240, China
e-mail: weilee@sjtu.edu.cn

against its transformation to martensite [17]. However, it is doubted that whether the compressive stress is retained in RA because the precipitation of carbides during tempering is associated with a volume contraction of martensite, which would reduce the compressive stress in RA [18]. Meanwhile, the thermal stability of RA after sub-zero Celsius treatment is also a controversial issue. Villa et al. [19] confirmed that the thermal stability of RA is decreased after sub-zero Celsius treatment through measuring the evolution of lattice strain in RA by synchrotron X-ray diffraction. Preciado et al. [20] presented the opposite result that sub-zero Celsius treatment could improve the thermal stability of RA. It is worth noting that the above-mentioned results were measured in either quenched or sub-zero Celsius treated conditions. However, quenched martensite is usually hard and brittle, so that tempering is necessary to increase the toughness of steel parts. Moreover, tempering is a complicated process which contains the carbon segregation, carbide precipitation and carbon partition from martensite into RA [21, 22]. Therefore, evaluating the thermal stability of RA by single heat treatment of quenched or sub-zero Celsius treatment is not enough. Meanwhile, there is no available literature about the effect of morphology on the mechanical stability of RA, which is also important in the manufacture processing of bearing steel.

This study aims at investigating the combined effect of sub-zero Celsius treatment and tempering on the mechanical and thermal stability of RA in bearing steel. The influence of carbon content, morphology and stress state on the stability of RA is discussed.

2 Materials and Methods

2.1 Materials and Microstructure Characterization

The material for the present study is GCr15 bearing steel with the chemical composition (wt%) of 1.05 C, 0.27 Si, 1.46 Cr, 0.33 Mn, 0.002 P and balance of Fe, which was supplied as spheroidized annealing condition. The specimens were subjected to two different heat treatment processes, as explained in the flowchart shown in Fig. 1. The specimens quenched into oil (50 °C) after austenitizing for 10 min at 860, 920 and 1150 °C, then tempered at 150 °C for 2 h. According to the austenitization temperature, the quenched–tempered specimens are denoted as 860QT, 920QT and 1150 QT. Sub-zero Celsius treatment was carried out in the mixtures of dry ice and ethanol at −65 °C for 30 min, which is in accordance with the temperature of bearing steel sub-zero Celsius treated in industry. The quenched sub-zero Celsius treated–tempered specimens are denoted as 860QST, 920QST and 1150QST.

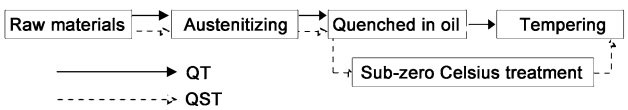

Fig. 1 Heat treatment processes for GCr15 bearing steel

Microstructures of the specimens were examined by scanning electron microscopy (SEM, JEOL, JSM-7600F). Specimens for SEM observation were prepared in the normal procedure and etched by 3% nital for 5 s.

2.2 Tensile Test and Magnetization Measurement

Tensile test specimens were prepared according to the ASTM standard (E 8M-13a) [23] with the long axes parallel to the rolling direction. Tensile test was performed at a displacement rate of 0.5 mm/min at room temperature using a Zwick universal testing machine. A standard knife-edge extensometer was used for all strain measurements. For each condition, one representative stress–strain curve was selected from three tests.

Specimens for magnetization measurements were cut by wire-electrode with a size of 2 mm × mm × 1.4 mm and measured in a Quantum Design Physical Property Measurement System [PPMS-9T (EC-II)]. The applied magnetic field was changed from 5 to 0 T in steps of 0.25 T at room temperature. The volume fraction of RA was calculated by the methods proposed by Zhao et al. [24]. The reference material is austenite-free specimen which was austenitized at 1050 °C for 0.5 h and furnace cooled to room temperature.

2.3 Residual Stresses Measurement

Residual stresses in RA were analyzed by XRD using the $\sin^2\Psi$ method [25]. The residual stresses of all austenite {311} specimens were measured on X-ray stress analyzer (Proto LXRD, Canada) with CrK_α radiation (30 kV, 25 mA, elastic constant of $1/2s_2 = 7.18 \times 10^{-6}$ MPa^{-1}; $1/2s_1 = 1.20 \times 10^{-6}$ MPa^{-1}) [26]. The $\sin^2\psi$ technique measurements were performed at eleven Psi tilt angles (β angles on the proto IXRD and LXRD, respectively). The range of β angle is −27° to 27° and recommended to add 3° oscillation at β angle to collect better peaks. To avoid surface interference, electrolytic etching with saturated NH_4OH solution was conducted under a voltage of 1.5 V [27].

2.4 DSC Experiment

Specimens for differential scanning calorimetry (DSC) measurements were cut by wire-electrode with a size of ϕ 4 mm × 0.7 mm and using a NETZSCH DSC 204F1

Phoenix thermal analysis apparatus applied for DSC detection, with Pt–Rh pan, and helium as protecting gas. DSC is calibrated by high purity In and Zn before commencement of measurements. An empty pan is used as the reference. The weight of sample is about 50–70 mg. Specimens were heated from room temperature to 450 °C at a heating rate of 5, 10, 15 and 20 °C/min.

The Kissinger-like method was used to obtain the activation energy (E) for the decomposition of RA, as follows [28, 29]:

$$\ln\left(T_{\mathrm{p}}^2/\phi\right) = E/(RT_{\mathrm{p}}) + A, \tag{1}$$

where R is the universal gas constant (8.314 J mol^{-1} K^{-1}), T_{p} is the peak temperature of transformation at each heating rate, ϕ is the heating rate, and A is a constant. When $\ln\left(T_{\mathrm{p}}^2/\phi\right)$ is plotted as a function of $1/T_{\mathrm{p}}$, the slope of the straight line obtained provides a value for the activation energy.

3 Results

Figure 2a shows the typical microstructures after traditional QT heat treatment (austenitizing temperature is 860 °C). It can be found that the microstructure consists of tempered martensite (M, dark, plate structure), RA (light constituent) and spherical carbides (SC). Figure 2b shows the microstructure of the specimen after QT treatment with the austenitizing temperature of 1150 °C. It is observed that the microstructure consists of tempered martensite and a large amount of RA (white regions). By comparing Fig. 2a, b, with increasing austenitizing temperature from 860 to 1150 °C, the SC disappeared and the morphology of RA changes from film-like to blocky [30]. After the sub-zero Celsius treatment, there is no noticeable change in microstructures by comparing Fig. 2a–d, respectively.

The fractions of RA are 13.2, 23.7 and 23.2 vol%, when austenitizing temperatures are 860, 920 and 1150 °C, respectively, as listed in Table 1. After sub-zero Celsius treatment, the fraction of RA decreases from 13.2 to 9.1 vol% as austenitization temperature is 860 °C, decreases from 23.7 to 11.3 vol% when austenitization temperature is 920 °C, and decreases from 23.2 to 10.1 vol% as austenitization temperature change to 1150 °C, respectively. The decreasing tendency of RA from QT to QST treatment indicates that sub-zero Celsius treatment promoted the RA to martensite transformation. Meanwhile, the elongation is decreased at higher austenitization temperature. The mechanical stability of RA is evaluated by the exponent decay law proposed by Sugimoto et al. [31, 32], as follows:

$$f_{\mathrm{RA}\varepsilon} = f_{\mathrm{RA0}} \cdot \exp(-k\varepsilon), \tag{2}$$

where $f_{\mathrm{RA}\varepsilon}$, f_{RA0} and k are the RA fraction at true strain ε, the initial RA fraction and the mechanical stability of RA, respectively. k is constant and a lower k corresponds to higher RA stability.

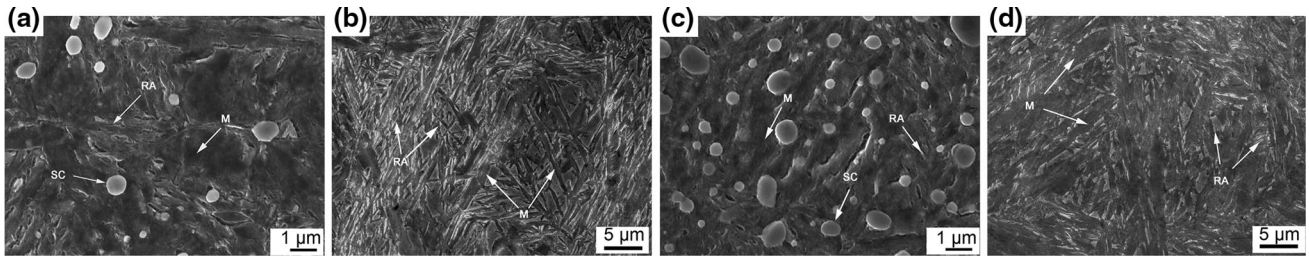

Fig. 2 SEM images of the specimens after QT and QST treatments, with austenitizing temperatures of 860 and 1150 °C: **a** 860 °C, QT; **b** 1150 °C, QT; **c** 860 °C, QST; **d** 1150 °C, QST

Table 1 Fraction and mechanical stability of RA for the specimens subjected to different treatments

Treatment	Fraction of RA_i (vol%)	Fraction of RA_f (vol%)	Elongation (%)	k
860QT	13.2	9.4	1.64	20.9
860QST	9.1	8.5	0.87	7.9
920QT	23.7	17.9	0.62	45.4
920QST	11.3	10.2	0.29	35.3
1150QT	23.2	F		
1150QST	10.1	F		

RA_i, the initial fraction of RA before tensile test; RA_f, the fraction of RA in fracture area after tensile test; F, failed before yielding; k, mechanical stability of RA

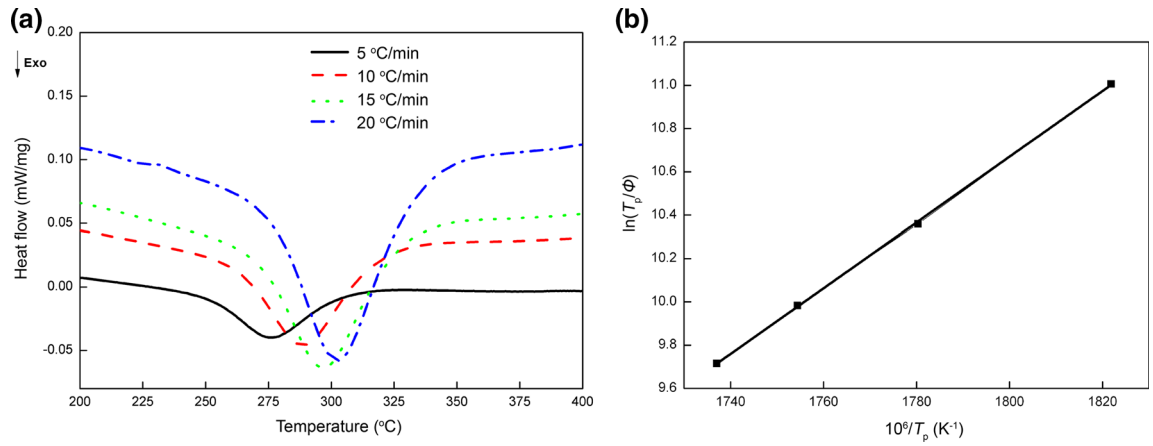

Fig. 3 **a** DSC curves of the QT specimen with austenitizing temperature of 860 °C at different heating rates of 5, 10, 15 and 20 °C/min; **b** determination of activation energy using Kissinger method

DSC can be utilized to determine the phase transformation temperatures and the activation energy of RA decomposition [33]. Figure 3 shows the DSC curves of the QT-treated specimen with austenitizing temperature of 860 °C at different heating rates of 5, 10, 15 and 20 °C/min and the activation energy calculated by the Kissinger method [34]. The DSC data and activation energy values are listed in Table 2. An exothermic peak was observed in the temperature range between 250 and 350 °C [20]. From Table 2, it can be found that both QT and QST specimens have the same phase transformation starting temperature (T_s) when austenitization temperatures are the same, and T_s slightly increases with austenitization temperature increase from 860 to 1150 °C. Meanwhile, the activation energy values for the decomposition of RA have the same tendency as T_s.

Figure 4 shows the hydrostatic compressive state of stress changes in RA measured by XRD using the $\sin^2\psi$ method. The level of compressive stress increased from 60 MPa of 860QT specimen to 235 MPa of 1150QT specimen. After sub-zero Celsius treatment, compressive stress in QST specimen is obviously higher than QT specimen. This result indicates that sub-zero Celsius treatment can create higher compressive stress in RA than traditional QT heat treatment. It is in accordance with synchrotron X-ray diffraction results in recent study [19, 35].

4 Discussion

The traditional heat treatment of GCr15 involves austenitization at relatively low temperature, resulting in incomplete dissolution of alloy carbides [36]. The higher austenitization temperature results in further dissolution of carbides, leaving a large amount of RA and more carbon content in RA at room temperature. Meanwhile, the film-like RA changed to block-like RA [30]. Calculations based on thermodynamic equilibrium conditions show that carbon content in RA increases from about 0.7 wt% to the nominal carbon contents of 1.05 wt% with austenitization temperature changes from 860 to 1150 °C.

4.1 Mechanical Stability

The stability of RA can be affected by its chemical composition [37], size [38] and morphology [39]. The

Table 2 Phase transformation starting temperature (T_s) and exothermic peak temperature (T_p) under heating rate of 5 °C/min and activation energy of different specimens

Treatment	T_s (°C)	T_p (°C)	Fraction of RA (vol%)	Activation energy (kJ/mol)
860QT	251	276	13.2	126.4 ± 0.15
860QST	252	275	9.1	129.3 ± 0.15
920QT	256	283	23.7	128.6 ± 0.15
920QST	255	285	11.3	130.2 ± 0.15
1150QT	262	290	23.2	131.8 ± 0.15
1150QST	261	290	10.1	136.5 ± 0.15

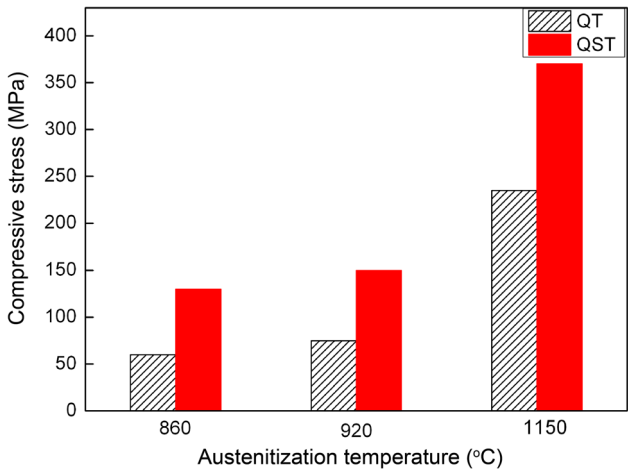

Fig. 4 Compressive stress in retained austenite of different specimens

decreasing tendency of elongation at higher austenitization temperature is due to the higher carbon content in martensite, and it is accompanied by the increasing microcrack tendency, although the volume fractions of RA is higher [40, 41]. However, the k value (see Table 1) is obviously increased at higher austenitization temperature. It is indicated that the mechanical stability of RA of 860QT specimen is higher than that of 920QT one. Results can be summarized that mechanical stability of RA is lower for specimens with higher austenitization temperature, although the carbon content in RA is higher (usually stable in thermodynamic). Therefore, the mechanical stability of RA is mainly attributed to the morphology which means that film-like RA provides better resistance to uniform strain (elongation) than that of blocky one. Similar results have been reported in a lower carbon steel [42].

In addition, the lower k value at QST specimen indicates that the mechanical stability of RA is improved after sub-zero Celsius treatment. There is no obvious difference in composition and morphology in both QT and QST specimens. But the higher compressive stress resided in RA at QST specimen, as shown in Fig. 4. The generation of compressive stress in RA due to martensite formation during sub-zero Celsius treatment was recognized recently [35]. On the other hand, the contraction of martensite due to the precipitation of carbides during tempering will impose an additional compression on RA. A relatively low fraction of austenite will be encapsulated by harder martensite, and the accumulated higher compressive stress in RA will be against strain-induced martensite transformation. Accordingly, sub-zero Celsius treatment could be exploited as an effective method to stabilize RA, and lower austenitization temperature should be chosen due to higher mechanical stability of RA in bearing steel.

4.2 Thermal Stability

Tempering was used to evaluate the thermal stability of RA, i.e., the decomposition of RA into ferrite and cementite [43]. The slightly increased T_s and activation energy, from 251 to 262 °C and from 126.4 to 131.8 kJ/mol (see Table 2), are due to the dissolution of more alloy carbides at higher austenitization temperature, and austenite stabilizing element such as chromium can shift the phase transformation temperature toward higher temperatures [44]. Another stabilizing factor is carbon, which is enriched up to 1.05 wt% for austenitization temperature of 1150 °C, and it can substantially improve the thermal stability.

In the case of identical austenitization temperature, the activation energy value in the QT specimens was around 128 kJ/mol and slightly higher values (approximately 130 kJ/mol) were measured for QST specimens which are close to the activation energy for the diffusion of C in austenite (129 kJ/mol) [40], suggesting that carbon diffusion in austenite is the rate-determining step for the decomposition of RA. It is well known that carbon partitioning may take place from martensite to RA during tempering [22]. More carbon partitioned in QT specimen than that of QST one, which is due to sub-zero Celsius treatment results in carbon segregation or clustering and makes more transitional carbides precipitate during subsequent tempering. The smaller activation energy in QT specimen is in well agreement with that the activation energy decreases, when the content of carbon increases [45].

On the other hand, the T_s of QT and QST specimens keeps the same. This is due to inhomogeneous carbon partitioning from martensite to RA during tempering. A part of RA kept the initial chemical composition (such as carbon contents) and decomposed at the early stage of decomposition, and thus, the T_s is unchanged for QT and QST specimen. Moreover, the effect of compressive stress in RA is weakened due to lattice expansion at temperature higher than 150 °C [19]. Therefore, the thermal stability of retained austenite is not related to compressive stress in RA, but is influenced by carbon partitioning.

5 Conclusions

(1) The sub-zero Celsius treatment and tempering can create higher compressive stress in retained austenite in high carbon GCr15 bearing steel than traditional quenched and tempering treatment, which is beneficial to the mechanical stability of retained austenite.
(2) Film-like retained austenite is more stable than that of block-like one, and thus, low austenitization

temperature is favorable in the manufacture of bearing steel.

(3) The thermal stability of retained austenite is influenced by the carbon partitioning during tempering.

Acknowledgments This work was financially supported by the National Basic Research Program of China (No. 2011CB706604) and National Natural Science Foundation of China (No. 51174251 and 51201105).

References

[1] J.R. Davis, K.M. Mills, S.R. Lampman, *Properties and Selection: Irons, Steels, and High-performance Alloys* (ASM International, Materials Park, 1990), pp. 167–213
[2] H.K.D.H. Bhadeshia, R.W.K. Honeycombe, *Steels: Microstructure and Properties* (Butterworth-Heinemann, Oxford, 2011), pp. 36–58
[3] H.K.D.H. Bhadeshia, Prog. Mater Sci. **57**, 268 (2012)
[4] E.S. Alley, R.W. Neu, Int. J. Fatigue **32**, 841 (2010)
[5] C.H. Surberg, P. Stratton, K. Lingenhöle, Cryogenics **48**, 42 (2008)
[6] A. Akhbarizadeh, A. Shafyei, M. Golozar, Mater. Des. **30**, 3259 (2009)
[7] D. Senthilkumar, I. Rajendran, M. Pellizzari, J. Siiriainen, J. Mater. Process. Technol. **211**, 396 (2011)
[8] M.A. Jaswin, D.M. Lal, A. Rajadurai, Tribol. Trans. **54**, 341 (2011)
[9] D. Mohan Lal, S. Renganarayanan, A. Kalanidhi, Cryogenics **41**, 149 (2001)
[10] A. Bensely, A. Prabhakaran, D. Mohan Lal, G. Nagarajan, Cryogenics **45**, 747 (2006)
[11] A. Molinari, M. Pellizzari, S. Gialanella, G. Straffelini, K.H. Stiasny, J. Mater. Process. Technol. **118**, 350 (2001)
[12] D. Das, A.K. Dutta, K.K. Ray, Wear **266**, 297 (2009)
[13] S. Zhirafar, A. Rezaeian, M. Pugh, J. Mater. Process. Technol. **186**, 298 (2007)
[14] D. Das, A.K. Dutta, K.K. Ray, Mater. Sci. Eng., A **527**, 2182 (2010)
[15] S. Gill, H. Singh, R. Singh, J. Singh, Int. J. Adv. Manuf. Technol. **48**, 175 (2010)
[16] S.S. Gill, J. Singh, R. Singh, H. Singh, Int. J. Adv. Manuf. Technol. **54**, 59 (2011)
[17] J.R. Patel, M. Cohen, Acta Metall. **1**, 531 (1953)
[18] K.Y. Golovchiner, Phys. Met. Metallogr. **37**, 126 (1974)
[19] M. Villa, K. Pantleon, M.A. Somers, Acta Mater. **65**, 383 (2014)
[20] M. Preciado, M. Pellizzari, J. Mater. Sci. **49**, 8183 (2014)
[21] Y. Ohmori, S. Sugisawa, Trans. Jpn. Inst. Met. **12**, 170 (1971)
[22] S. Matas, R. Hehemann, Nature **187**, 685 (1960)
[23] Subcommittee, ASTM E8/E8M-13a, 2013
[24] L. Zhao, N. Van Dijk, E. Brück, J. Sietsma, S. Van der Zwaag, Mater. Sci. Eng. A **313**, 145 (2001)
[25] I.C. Noyan, J.B. Cohen, *Residual Stress: Measurement by Diffraction and Interpretation* (Springer, New York, 1987)
[26] Q. Feng, C. Jiang, Z. Xu, Mater. Des. **47**, 68 (2013)
[27] I. Zucato, M.C. Moreira, I.F. Machado, S.M.G. Lebrão, Mater. Res. **5**, 385 (2002)
[28] H.E. Kissinger, Analyt. Chem. **29**, 1702 (1957)
[29] E.J. Mittemeijer, J. Mater. Sci. **27**, 3977 (1992)
[30] H. Luo, J.J. Liu, B.L. Zhu, Wear **174**, 57 (1994)
[31] K.I. Sugimoto, M. Kobayashi, S.I. Hashimoto, Metall. Trans. A **23**, 3085 (1992)
[32] J. Shi, X. Sun, M. Wang, W. Hui, H. Dong, W. Cao, Scr. Mater. **63**, 815 (2010)
[33] M. Van Rooyen, E. Mittemeijer, Scr. Metall. **16**, 1255 (1982)
[34] E. Mittemeijer, J. Mater. Sci. **27**, 3977 (1992)
[35] M. Villa, F.B. Grumsen, K. Pantleon, M.A. Somers, Scr. Mater. **67**, 621 (2012)
[36] G. Thomas, Metall. Trans. A **9**, 439 (1978)
[37V Y. Tomita, T. Okawa, Mater. Sci. Eng., A **172**, 145 (1993)
[38] H.S. Yang, H. Bhadeshia, Scr. Mater. **60**, 493 (2009)
[39] I.B. Timokhina, P.D. Hodgson, E.V. Pereloma, Metall. Mater. Trans. A **35**, 2331 (2004)
[40] K. Nakazawa, G. Krauss, Metall. Trans. A **9**, 681 (1978)
[41] G. Krauss, Mater. Sci. Eng., A **273**, 40 (1999)
[42] X. Xiong, B. Chen, M. Huang, J. Wang, L. Wang, Scr. Mater. **68**, 321 (2013)
[43] P. Morra, A. Böttger, E. Mittemeijer, J. Therm. Anal. Calorim. **64**, 905 (2001)
[44] W. Shi, L. Li, B.C. De Cooman, P. Wollants, C.X. Yang, J. Iron. Steel Res. Int. **15**, 61 (2008)
[45] W. Batz, R.F. Mechl, Trans. AIME **188**, 553 (1950)